

Oxygen-induced exchange-coupling reversal at the Mn-Co interface

W. L. O'Brien

Synchrotron Radiation Center, University of Wisconsin-Madison, 3731 Schneider Drive, Stoughton, Wisconsin 53589

B. P. Tonner

Department of Physics, University of Wisconsin-Milwaukee, 1900 East Kenwood Boulevard, Milwaukee, Wisconsin 53211

(Received 27 October 1997)

We report on a phenomenon associated with surface magnetism: the reversal of exchange coupling induced by oxidation. Ferromagnetically ordered submonolayer films of Mn grown on fcc Co(001) have their magnetization direction oriented parallel to the Co magnetization. After oxygen exposure the Mn atoms remain ferromagnetically ordered but their magnetization direction rotates 180° and is now aligned antiparallel to the Co magnetization. This behavior in magnetic coupling between the Mn and Co films is not consistent with recent theoretical predictions. This difference is perceived to lie in the atomic scale morphology at the Mn-Co interface. [S0163-1829(98)03630-3]

INTRODUCTION

Monolayer films are often found to order ferromagnetically when grown on ferromagnetic substrates.¹⁻⁹ This is true even for films that do not possess ferromagnetic order when in the bulk phase. Recently, much experimental¹⁻⁶ and theoretical⁷⁻⁹ effort has been expended in measuring and predicting the magnetic ordering in these overlayers. This interest has been brought about in part by advances in x-ray magnetic circular dichroism (XMCD). XMCD gives element-specific magnetic-ordering information¹⁻² that allows the magnetic ordering of the overlayer to be distinguished from the magnetic ordering of the substrate. XMCD also has the required sensitivity for the measurement of single monolayer or thinner films.^{1,2} Simultaneous with the growing application of XMCD, the theory of electronic structure has reached a stage where questions regarding the type of magnetic ordering in monolayer films can accurately be determined.⁸

An important question regarding these ferromagnetic monolayers is whether they are oriented with their magnetization parallel or antiparallel to the magnetization of the substrate. For Mn films, ferromagnetic ordering has been observed for growth on a number of different substrates, but the sign of the magnetic coupling depends on the substrate. Monolayer films of Mn grown on fcc Co(001) (Ref. 1) and fcc Ni(001) (Ref. 2) have their magnetization oriented parallel to the magnetization of the substrate. For growth on Ni(001) a $\frac{1}{2}$ -ML film of Mn forms the MnNi $c(2 \times 2)$ surface alloy that is ferromagnetically ordered.² The magnetic alignment of ferromagnetic Mn films on bcc Fe is controversial with reports of both antiparallel³⁻⁵ and parallel⁶ alignment to the magnetization of the Fe.

A recent theoretical investigation⁷ of the magnetic ordering of a single monolayer of Mn/Co(001) is in disagreement with experiment.¹ Using a tight-binding Hubbard-type Hamiltonian, Noguera *et al.*⁷ found two stable solutions for the magnetic ordering in Mn/Co. In the first solution the Mn atoms are ferromagnetically ordered, but their magnetization is oriented antiparallel to the magnetization of the Co sub-

strate. In the second solution the Mn atoms are antiferromagnetically ordered and the surface undergoes a $c(2 \times 2)$ reconstruction. Experimental studies¹ of Mn/Co show ferromagnetic ordering in the Mn overlayer with the Mn magnetization oriented parallel to the magnetization of the Co substrate. This configuration does not give a stable solution in the theoretical analysis. It is clear that the magnetic interaction across the Mn/Co interface deserves more attention.

In this paper we report on a surface phenomenon associated with the magnetic alignment of ferromagnetic Mn/Co films and the effects of oxidation. We begin by repeating earlier measurements on a $\frac{1}{2}$ -ML Mn film grown on an fcc Co(001) substrate.¹ XMCD is used to obtain element-specific magnetic ordering information and element-specific hysteresis behavior. Measurements show that a $\frac{1}{2}$ -ML film of Mn grown on Co is ferromagnetically ordered and aligned parallel to the magnetization of the Co substrate. After exposure to 3 langmuirs ($1 \text{ L} = 10^{-6} \text{ Torr sec}$) O_2 the Mn and Co films each remained ferromagnetically ordered, but the coupling between the Mn and Co films rotates 180° and becomes antiparallel.

EXPERIMENT

The fcc Co substrate was grown as a 5-ML film on a clean Cu(001) single crystal using electron-beam evaporation. The Cu(001) surface was prepared by sputter and annealing cycles with an annealing temperature of 900 K. The Mn films were grown by evaporating pure Mn from an Al_2O_3 crucible. Deposition rates were 1 ML/min for Co and $\frac{1}{2}$ ML/min for Mn as determined by a calibrated quartz-crystal oscillator. The quartz-crystal oscillator was calibrated by observing the intensity of the $c(2 \times 2)$ electron-diffraction spots while growing Mn on Cu(001) and Ni(001). The $c(2 \times 2)$ diffraction spots have their maximum intensity at $\frac{1}{2}$ -ML coverage of Mn.² The base pressure of the experimental chamber was 1×10^{-10} Torr that did not rise above 2×10^{-10} Torr during film growth. Low-energy electron diffraction (LEED) was used to study film growth and to align

the sample prior to the magnetization measurements. After deposition of 5 ML of Co, a $p(1 \times 1)$ LEED pattern, identical to that of the Cu(001) substrate, was observed. This is consistent with the well-known growth of metastable fcc Co(001) on Cu(001).¹⁰ Addition of $\frac{1}{2}$ -ML Mn did not alter the LEED pattern.

The samples were studied *in situ* by XMCD using the 10-m toroidal grating monochromator located at the Synchrotron Radiation Center.¹¹ The magnetic dichroism signal, $\sigma_M = \sigma_+ - \sigma_-$, is the difference between the x-ray-absorption spectrum with the photon spin parallel (σ_+) and antiparallel (σ_-) to the sample magnetization. Absorption measurements were made by total electron yield and corrected for saturation using the analysis of Ref. 12. The XMCD spectra were obtained using circularly polarized light with a constant degree of circular polarization, $P_c = 0.85$, by flipping the sample magnetization direction at each photon energy. The dichroism spectra were normalized by first subtracting an E^{-n} background from the σ_+ and σ_- spectra and then normalizing the edge jump in $(\sigma_+ + \sigma_-)$ to unity. This normalizes the dichroism intensity to a per atom basis that is useful for comparisons involving the dichroism sum rules. Spectra were corrected for incident photon flux by simultaneously measuring the photoemission intensity from a Ni grid (90% transmission). Dichroism spectra were obtained with the films in their remanent magnetic state. Element-specific hysteresis curves¹³ were obtained by setting the photon energy at either the Mn L_3 (641.4 eV) or Co L_3 (779.7 eV) absorption maximum and sweeping the applied magnetic field.

While the results presented in this paper were obtained using $\frac{1}{2}$ -ML Mn films, identical results were obtained for a $\frac{1}{4}$ -ML film of Mn/Co(001). The lower coverage films were studied in order to minimize the possibility of three-dimensional growth. Details of the dichroism measurements can be found in Ref. 13.

RESULTS AND DISCUSSION

In Fig. 1 we show the Mn and Co $L_{2,3}$ XMCD spectra for a $\frac{1}{2}$ -ML film of Mn grown on fcc Co(001), both before and after exposure to 3 L of oxygen. The presence of a nonzero intensity in the Mn and Co XMCD spectra shows that both the Mn and Co are ferromagnetically ordered. The sign of the Mn and Co L_3 XMCD white lines are both negative, showing that the magnetization of the Mn film is aligned parallel to the magnetization of the substrate. After oxidation the sign of the Mn XMCD spectra is reversed and the L_3 and L_2 features are resolved into a number of peaks. Both the Mn and Co layers are still ferromagnetically ordered, but oxidation rotates the spin orientation of the Mn overlayer 180° relative to the spin orientation of the Co substrate. The coupling between the Mn and Co is now antiparallel.

Hysteresis curves for both Mn and Co were obtained for different oxygen exposures between 0 and 3 L. This was accomplished by repeatedly raising the chamber pressure to 5×10^{-9} Torr oxygen for a specific time, pumping the chamber out, and then measuring the hysteresis curves. For each exposure level the Co and Mn hysteresis curves were similar in shape: they were both nearly square and had the same coercive field. Figure 2 shows the coercive field dependence

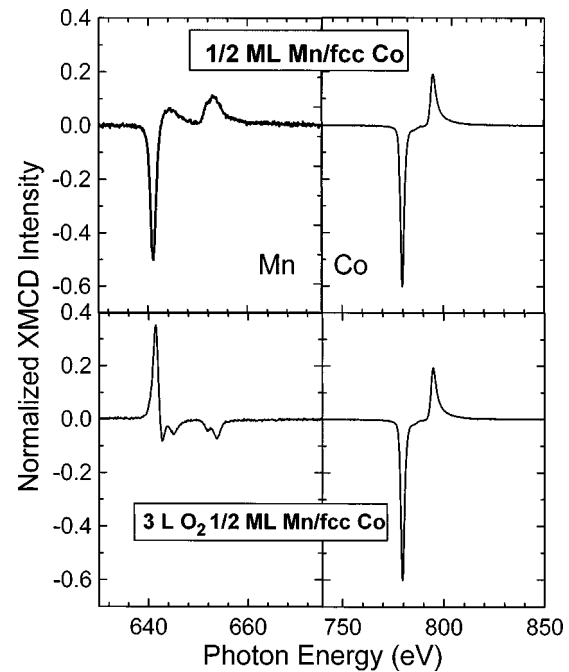


FIG. 1. Mn $L_{2,3}$ and Co $L_{2,3}$ XMCD spectra for a $\frac{1}{2}$ -ML Mn film grown on a 5-ML fcc Co substrate, top, and the same film after exposure to 3-L O_2 , bottom. Before oxidation both the Mn and Co films are ferromagnetically ordered and the Mn magnetization is aligned parallel to the Co. After oxidation the Mn and Co films each remain ferromagnetically ordered but they are now aligned antiparallel. Spectra are normalized such that $(\sigma_+ + \sigma_-) = 1$, 30 eV above the L_2 edge.

on oxygen exposure. The coercivity remains nearly constant at 12 Oe between 0 and 2 L of exposure, then it increases up to 28 Oe after 3 L of exposure. In the inset of Fig. 2 we show representative Mn and Co hysteresis curves. Before oxidation the Mn hysteresis curve has the exact shape as the Co hysteresis curve. These curves are also identical to the Co

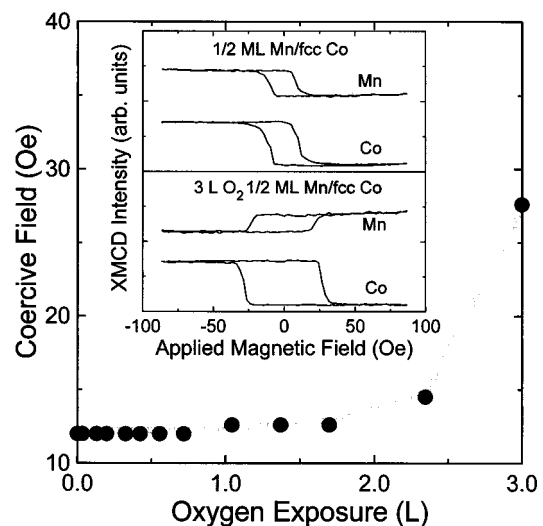


FIG. 2. Coercive field of a $\frac{1}{2}$ -ML Mn/Co bilayer vs oxygen exposure. Inset: Mn and Co element specific hysteresis curves obtained before oxidation and after exposure to 3-L O_2 . The curves were obtained by setting the photon energy at the Mn and Co L_3 absorption maximum.

hysteresis curve obtained before the addition of Mn. This shows that the ferromagnetic ordering in the Mn film is induced by exchange coupling to the Co substrate and the coupling constant is positive. After exposure to 3 L O₂ the Co and Mn hysteresis curves change. The coercive field increases and the sign of the Mn hysteresis curve is reversed. The switching fields for the Co and Mn are still the same, implying the magnetic ordering in the Mn film is induced by exchange coupling to the Co substrate but the sign of the coupling is now negative.

XMCD spectra of the type shown in Fig. 1 have been used to accurately determine both the spin m_{spin} and orbital m_{orb} contributions to the total magnetic moment m_{tot} .¹⁴ This analysis requires the use of the dichroism sum rules¹⁵ that describe m_{spin} and m_{orb} in terms of the integrated L_3 and L_2 dichroism intensities. In our measurements of the Mn XMCD spectra we found that the Mn absorption line shape changed during the measurement. This led to large uncertainties in the calculated values of m_{spin} and m_{orb} . It appears that Mn reacts with the background gas (1×10^{-10} Torr) during the measurement. In fact, for a very thin Mn film, 0.15 ML, the magnetic coupling between Mn and Co reversed after sitting for 1 h in the vacuum chamber at 1×10^{-10} Torr. Accompanying this reversal was a change in the Mn XMCD line shape similar to the change found after oxidizing the $\frac{1}{2}$ -ML film, Fig. 1. Clearly the Mn film is very reactive even to the residual gas remaining in a UHV environment and the magnetic properties of the Mn are altered. This high reactivity made it impractical for us to measure m_{spin} and m_{orb} for Mn versus oxygen exposure using the dichroism sum-rule analysis. Contrary to this, the Co absorption spectra did not measurably change with oxygen exposure.

In order to measure the changes in the Mn and Co moments versus oxygen exposure, a quicker method was needed. A reasonable estimate for the magnetic moment can be obtained using the normalized dichroism intensity measured at the L_3 white-line maximum.¹³ Such a measurement can be performed rapidly, minimizing the effects due to the background pressure. The normalized dichroism intensity at L_3 , $\Sigma_n(L_3)$, is defined as

$$\Sigma_n(L_3) = \sigma_M(L_3) / [\sigma_+(L_3) + \sigma_-(L_3)], \quad (1)$$

where $\sigma_+(L_3) + \sigma_-(L_3)$ is a good approximation to the total absorption intensity at the L_3 white-line maximum. If the orbital moment is assumed to be zero and if the absorption line shapes do not change then

$$m_{\text{tot}} = C \Sigma(L_3), \quad (2)$$

where C is a constant that we have determined by measuring $\Sigma(L_3)$ for a thick (40-Å) film of Co/Cu(001) and using $m_{\text{tot}}(\text{Co}) = 1.67 \mu_B$, $C = 0.108 \mu_B$. Values for the Co moment versus oxygen exposure obtained in this manner are presented in Fig. 3. Oxygen exposure levels between 0 and 3 L have no effect on the Co moment.

Deriving the Mn moments dependence on oxygen exposure is more uncertain. First of all, the Mn absorption line shape is very dependent on oxygen exposure, Fig. 1. Furthermore, the value for the constant C in Eq. (2) depends on which element is being considered. We have estimated the value of the constant C for Mn from the value of the constant

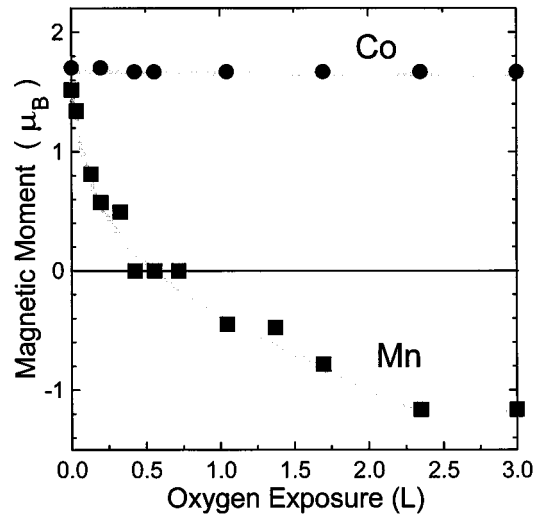


FIG. 3. Average magnetic moments of Co and Mn atoms in a $\frac{1}{2}$ -ML Mn/5-ML Co bilayer vs oxygen exposure.

C obtained for Co using the transferability concept as first proposed by Samant *et al.*¹⁶ Using this method, values for the average Mn moment versus oxygen exposure were obtained and are presented in Fig. 3. The Mn moment vanishes after exposure to $\frac{1}{2}$ L of oxygen, but reappears after 1-L exposure, but is now oriented in the opposite direction with respect to the Co magnetization.

To quantify the effects of oxidation on the electronic environment of Mn we compare the Mn dichroism and x-ray-absorption spectra (XAS) to theoretical calculations, Fig. 4. The theoretical calculations are for a $\text{Mn}^{+2} d^5 S = \frac{5}{2}$ atom¹⁷ and we have used $\sigma_+ + \sigma_-$ for the experimental XAS. There

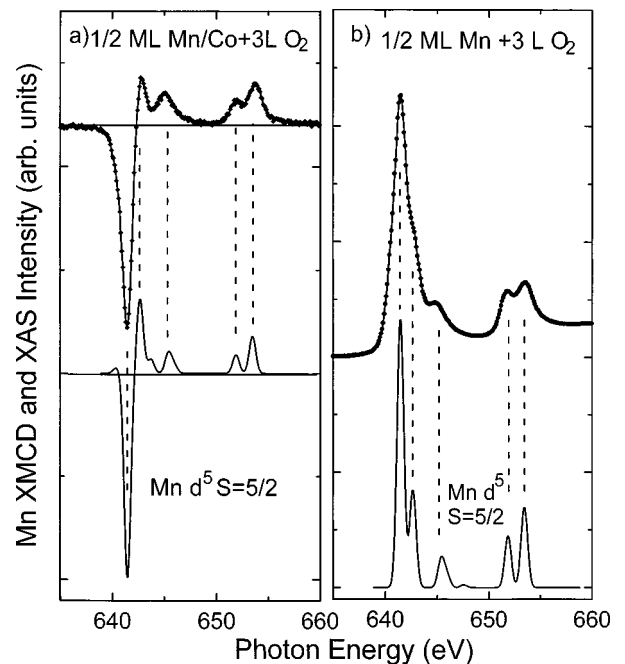


FIG. 4. Comparison of (a) Mn $L_{2,3}$ XMCD spectra and (b) XAS spectra for the $\frac{1}{2}$ -ML Mn film after oxidation to the spectra for a $\text{Mn}^{+2} d^5 S = \frac{5}{2}$ state (Ref. 17). Excellent agreement is found between the experimental spectra and the theoretical results of Ref. 17.

is excellent agreement between the atomic calculation and experimental spectra of the oxidized film with 3-L exposure. Based on the comparisons in Figs. 1–4, exposure to oxygen converts Mn into an almost pure $\text{Mn}^{+2} d^5 S = \frac{5}{2}$ state, as would be expected based on electronegativity arguments. The oxygen reacts primarily with Mn forming a MnO_x compound on the Co surface. The exact oxygen concentration is not known but the comparison in Fig. 4 suggests that $x \sim 1$.

Changes in magnetic switching behavior due to oxygen exposure, Fig. 2, have been observed for other thin-film systems. For thin Co films grown on miscut Cu(001), exposure to oxygen causes a 90° rotation in the step-induced uniaxial anisotropy.¹⁸ The mechanism behind this rotation is believed to be a change in the magnetic surface anisotropy of the step site atoms. Magnetic anisotropies result from the spin-orbit interaction and are due to anisotropies in m_{orb} .¹⁹ It is possible that oxygen-induced changes in the anisotropy of m_{orb} are responsible for the change in the coercive field of the film. In order to check whether the changes in coercive field, Fig. 2, are connected to a change in m_{orb} , we have performed detailed analysis of the Co XMCD spectra both before and after oxygen exposure. The orbital moment can be calculated from the integrated dichroism intensity¹⁶

$$m_{\text{orb}} = \frac{\int \sigma_M d\omega}{B|M_{pd}|^2}, \quad (3)$$

where B is a constant dependent on the angular momenta of the core hole and valence shell involved in the dipole transition, $|M_{pd}|^2$ is the dipole matrix element, and the integral is over the L_3 and L_2 dichroism spectra. $B|M_{pd}|^2$ is a constant for any particular element and can be determined by integrating σ_M for a sample with a known m_{orb} .¹⁶ We have measured $B|M_{pd}|^2$ for a 40-Å Co film grown on Cu(001) assuming $m_{\text{orb}} = 0.147\mu_B$. We find $B|M_{pd}|^2 = 4.1\mu_B^{-1} \pm 3\%$ determined by multiple measurements on the same sample. The 3% uncertainty arises from the experimental spread in these results. Using this value we find that the average orbital moment for the Co atoms is $0.150\mu_B \pm 5\%$ before oxidation, and $0.155\mu_B \pm 5\%$ after oxidation. These values are for magnetization along the easy axis, the (110) direction. Measurements of m_{orb} for magnetization along the in-plane hard axis, (100) direction, contained large uncertainties due to the necessity of measuring electron yield in an applied field. This made it impractical to measure the anisotropy in the orbital moment.

The measured change in the Co orbital moment due to oxygen exposure is within our experimental uncertainty. For comparison, Weller *et al.*¹⁹ found a factor of 2 change in the orbital moment for a 5-ML film of Co grown on Au(111) for different magnetization directions. This factor of 2 change is responsible for the magnetocrystalline anisotropy, which in turn determines the easy axis of magnetization for Co/Au. For the Mn/Co bilayer, 3 L of oxygen exposure has no measurable effect on the magnetic moment of Co; neither the orbital moment, nor the total moment, Fig. 2, are effected. Furthermore, neither the XAS nor the XMCD spectra of Co are effected by exposure to 3 L of oxygen. Based on these findings we believe that any anisotropy in the orbital moment of Co is not affected by oxidation. The increase in the coer-

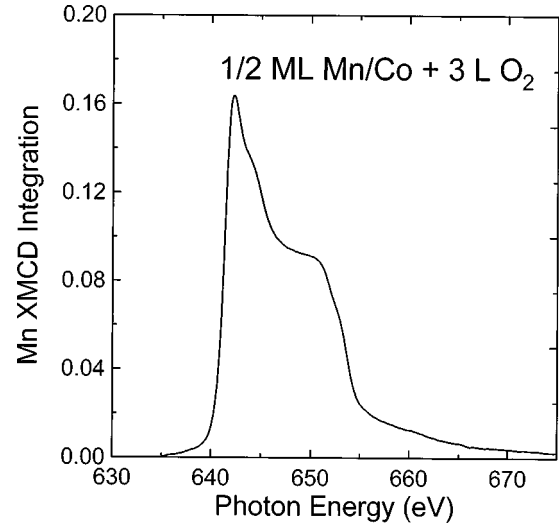


FIG. 5. Integration of normalized Mn XMCD spectra obtained after exposure to 3-L O_2 . According to the dichroism sum rules, Ref. 15, this integral is equal to the Mn orbital moment that approaches zero.

cive field of the Co/Mn bilayer with oxygen exposure is not due to oxidation effects of Co.

Since oxygen does react with Mn it is appropriate to examine the orbital moment of Mn to see if this could explain changes in the magnetic switching behavior of the bilayer. As stated earlier it was impractical to measure m_{orb} for Mn versus oxygen exposure due to the line-shape changes. However, after 3 L of oxygen exposure, the Mn XMCD spectra were stable, in that sequential scans were identical. In order to calculate m_{orb} from the Mn XMCD spectra a value for $B|M_{pd}|^2$ was needed for Mn. We could not repeat the method used for determining $B|M_{pd}|^2$ for Co since there is no suitable source of ferromagnetic Mn. However, we can estimate $B|M_{pd}|^2$ for Mn, using the transferability concept proposed by Samant *et al.*¹⁶ by assuming it is equal to $B|M_{pd}|^2$ for Co. This assumption adds an additional 20% uncertainty to the value of m_{orb} .¹⁶ In this manner we calculate that m_{orb} for Mn is $< 0.005\mu_B$. The results of the Mn XMCD integration is given in Fig. 5, which clearly shows how the total dichroism intensity and therefore m_{orb} is approximately zero. A value of m_{orb} equal to zero is consistent with Mn being in the $d^5 S = \frac{5}{2}$ state.

All evidence points to the oxidized Mn being predominantly in the d^5 Hund's rule ground state. Although our XMCD studies of the unoxidized Mn did not yield a value for the orbital moment, it was clear that it was not equal to zero and therefore oxidation did affect the orbital moment of Mn. By inducing a change in the orbital moment it is reasonable to assume that oxidation also changes the anisotropy in the orbital moment of Mn. However, we do not believe that this change is responsible for the increase in coercive field. In the d^5 Hund's rule ground state there is no orbital moment, $\langle l_z \rangle = 0$, and the magnetization direction for Mn is due purely to exchange coupling. Anisotropies in orbital moments are caused by changes in the crystal fields quenching of the orbital moment for different magnetization directions. If Mn is in the pure Hund's rule ground state, there can be no anisotropy in the orbital moment since it is equivalent to

zero. If we assume that oxidation results predominantly in the Mn $d^5 S = \frac{5}{2}$ state, then anisotropies due to the spin-orbit interaction should be lower after oxidation, and the oxidized Mn film should rotate at a lower applied field. This is opposite to what we find.

An alternative mechanism for the increase in coercivity with oxygen exposure is therefore needed. It is well known that misfit dislocations increase the coercive field of bulk materials by applying a frictional force to domain-wall motion.²⁰ Recently this relationship has been extended to thin films.²¹ The stress in pseudomorphic films increases with thickness until it becomes thermodynamically favorable to form misfit dislocations. The thickness at which this occurs is the critical thickness for pseudomorphic growth, t_c . The onset of misfit dislocations at t_c is, for many films, accompanied by a large increase in the coercive field.²¹ The important parameter in determining t_c is the lattice misfit $\eta = (a_0 - a_s)/a_s$, where a_s and a_0 are the lattice parameters of the substrate and overlayer, respectively. For Mn/Co $\eta = -4.7\%$, while for MnO/Co $\eta = -13\%$. Using these values and the analysis of Matthews and Crawford,²² t_c for Mn/Co is 4 ML while t_c for MnO/Co is <1 ML. Therefore, deposition of $\frac{1}{2}$ ML of Mn on Co should have no effect on the coercivity while forming <1 ML of MnO on Co should increase the stress in the film enough to form misfit dislocations and increase the coercive field. This is exactly the behavior we have found, suggesting that strain release in the MnO layer is responsible for the increase in coercive field with oxygen exposure.

The magnetic coupling across the unoxidized Mn/Co interface is opposite to that predicted by theory;⁷ however, the theoretical calculations were performed on a perfect interface, which by definition has no intermixing or three-dimensional growth. Since nonideal morphology is known to modify the magnetic ordering across an interface,^{9,23,24} we must consider the possibility that the effects of intermixing, islanding, or changes in interlayer lattice constant⁹ could be responsible for the disagreement with theory. To our knowledge, no atomic scale morphology measurements have yet been performed on this interface but we can use thermodynamic arguments as a guide to determining the expected growth mode. Mn has a lower surface free energy than Co, and Mn and Co are miscible (low interface free energy). This suggests that the first ML of Mn wets the Co surface so that there is no islanding for submonolayer coverages. However, the low interface free energy in combination with low surface free energy of Mn suggests that formation of a surface alloy is thermodynamically stable.

Mn does form a surface alloy with both Ni and Cu,²⁵ and the MnNi surface alloy exhibits some unusual magnetic

properties.² The MnNi and MnCu surface alloys form a $c(2 \times 2)$ superlattice as determined by LEED.^{2,25} If a MnCo surface alloy forms it lacks long-range site ordering of the Mn atoms since no superlattice diffraction pattern was observed by LEED. The formation of a MnCo surface alloy, which is consistent with free-energy arguments, may explain the disagreement in the theoretical and experimental exchange coupling between Mn and Co. The reversal in exchange coupling upon oxidation is even less understood.

SUMMARY

Mn and MnO are both antiferromagnets as bulk materials. When grown as a single layer on the fcc Co(001) surface both Mn and oxygen-exposed Mn layers order ferromagnetically, with their magnetization parallel to the Co magnetization for Mn and antiparallel for oxygen-exposed Mn. In both cases the Mn and Co hysteresis behavior shows that the magnetic ordering in the Mn films is induced by exchange coupling across the Mn/Co interface. The sign of the exchange coupling is positive for the as-grown bilayer and switches to negative after exposure to 1-L O₂. The exchange coupling between the unoxidized Mn/Co interface is not explained by theoretical analysis of a perfect interface. Thermodynamic arguments suggest intermixing of Mn and Co in the first layer with the possible formation of a substitutionally disordered surface alloy. The formation of such an alloy could explain the disagreement between theory and experiment for the unoxidized Mn/Co interface. The reversal in the exchange coupling between Mn and Co upon oxidation is a new phenomenon and is not fully understood.

Exposure to oxygen also increases the coercivity of the Mn/Co bilayer. This increase is not due to changes in orbital moment anisotropies. Analysis of the Mn XMCD and XAS spectra show that Mn is in the d^5 Hund's rule ground state after exposure to 3-L O₂, $\langle l_z \rangle = 0$. This is verified by a detailed analysis of the Mn XMCD spectra after oxidation, which shows that $m_{\text{orb}} < 0.005 \mu_B$ for Mn. Also, exposure to 3-L O₂ has no effect on the orbital or spin moment of the underlying Co layer. The increase in coercivity with oxygen exposure is due to the large strain present in the MnO/Co bilayer due to the large, 13%, lattice mismatch between MnO and Co.

ACKNOWLEDGMENT

This work was based upon research conducted at the Synchrotron Radiation Center, University of Wisconsin-Madison which is supported by the NSF under Award No. DMR-95-31009.

¹W. L. O'Brien and B. P. Tonner, Phys. Rev. B **50**, 2963 (1994).

²W. L. O'Brien and B. P. Tonner, Phys. Rev. B **51**, 617 (1995).

³C. Roth, T. Kleemann, F. U. Hillebrecht, and E. Kisker, Phys. Rev. B **52**, R15 691 (1995).

⁴O. Rader, W. Gudat, D. Schmitz, C. Carbone, and W. Eberhardt, Phys. Rev. B **56**, 5461 (1997).

⁵J. Dresselhaus, D. Spanke, F. U. Hillebrecht, E. Kisker, G. van

der Laan, J. B. Goedkoop, and N. B. Brooks, Phys. Rev. B **56**, 5461 (1997).

⁶S. Andrieu, M. Finazzi, Ph. Bauer, H. Fischer, P. Lefevre, A. Traverse, K. Hricovini, G. Krill, and M. Piecuch, Phys. Rev. B **57**, 1985 (1998).

⁷A. Noguera, S. Bouarab, A. Mokrani, C. Demangeat, and H. Dreyse, J. Magn. Mater. **156**, 21 (1996).

- ⁸S. Mirbt, O. Eriksson, B. Johansson, and H. L. Skriver, Phys. Rev. B **52**, 15 070 (1995).
- ⁹R. Wu and A. J. Freeman, Phys. Rev. B **51**, 17 131 (1995).
- ¹⁰H. Li and B. P. Tonner, Phys. Rev. B **40**, 10 241 (1989).
- ¹¹R. W. C. Hansen, W. L. O'Brien, and B. P. Tonner, Nucl. Instrum. Methods Phys. Res. A **347**, 148 (1994).
- ¹²W. L. O'Brien and B. P. Tonner, Phys. Rev. B **50**, 12 672 (1994).
- ¹³W. L. O'Brien and B. P. Tonner, Phys. Rev. B **52**, 15 332 (1995).
- ¹⁴C. T. Chen, Y. U. Idzerda, H.-J. Lin, N. V. Smith, G. Meigs, E. Chaban, G. H. Ho, E. Pellgrin, and F. Sette, Phys. Rev. Lett. **75**, 152 (1995).
- ¹⁵P. Carra, B. T. Thole, M. Altarelli, and X. Wang, Phys. Rev. Lett. **70**, 694 (1993).
- ¹⁶M. G. Samant, J. Stöhr, S. S. P. Parkin, G. A. Held, B. D. Hermsmeier, F. Herman, M. van Schilfgaarde, L.-C. Duda, D. C. Mancini, N. Wassdahl, and R. Nakajima, Phys. Rev. Lett. **72**, 1112 (1994).
- ¹⁷B. T. Thole and G. van der Laan, Phys. Rev. B **38**, 3158 (1988); G. van der Laan and B. T. Thole, *ibid.* **43**, 13 401 (1991).
- ¹⁸W. Weber, C. H. Back, U. Ramsperger, A. Vaterlaus, and R. Allenspach, Phys. Rev. B **52**, R14 400 (1995).
- ¹⁹D. Weller, J. Stöhr, R. Nakajima, A. Carl, M. G. Samant, C. Chappert, R. Megy, P. Beauvillain, P. Beillet, and G. A. Held, Phys. Rev. Lett. **75**, 3752 (1995).
- ²⁰Chih-Wen Chen, *Magnetism and Metallurgy of Soft Magnetic Materials* (General Publishing, Ontario, 1986), pp. 286–295.
- ²¹W. L. O'Brien and B. P. Tonner, Phys. Rev. B **54**, 9297 (1996).
- ²²J. W. Matthew and J. L. Crawford, Thin Solid Films **5**, 187 (1970).
- ²³R. Coehoorn, J. Magn. Magn. Mater. **151**, 341 (1995).
- ²⁴M. M. Schwickert, R. Coehoorn, M. A. Tomaz, D. Lederman, E. Mayo, W. L. O'Brien, Tao Lin, and G. R. Harp (unpublished).
- ²⁵M. Wuttig, C. C. Knight, T. Flores, and Y. Gauthier, Surf. Sci. **292**, 189 (1993).